JOURNAL OF THERMOPHYSICS AND HEAT TRANSFER
Vol. 9, No. 4, October–December 1995

Effect of Spray Characteristics on Spray Cooling with Liquid Nitrogen

Maninder S. Sehmbey,* Louis C. Chow,† Ottfried J. Hahn,‡ and Martin R. Pais§
University of Kentucky, Lexington, Kentucky 40506

Operation of power electronics at liquid nitrogen (LN2) temperature is a very attractive possibility. However, a high heat flux (over 100 W/cm²) cooling technique like spray cooling will have to be used to realize all the advantages of low-temperature operation. This study provides empirical correlations for LN2 spray cooling. A general semiempirical correlation (based on macrolayer dryout model) for spray cooling critical heat flux (CHF) is obtained. This correlation is shown to be very accurate for predicting spray cooling CHF for different liquids and spray conditions. An empirical correlation for heat flux is also presented. This study also shows the importance of surface roughness for spray cooling with liquid nitrogen. The rougher surfaces were shown to have significantly higher heat transfer rates and similar CHFs occurring at lower temperatures.

Nomenclature

C_l = liquid specific heat at constant pressure, J/kg·K
D = hydraulic diameter of heater surface, m
d = diameter of a droplet in a spray sample, m
d_d = diameter of the liquid disc formed by an impinging drop, m
d_{20} = surface mean diameter of spray, $(\Sigma\, d^2/N_t)^{1/2}$, m
d_{30} = volume mean diameter of spray, $(\Sigma\, d^3/N_t)^{1/3}$, m
d_{32} = Sauter mean diameter of spray, $(\Sigma\, d^3/\Sigma\, d^2)$, m
G = mass flow rate per unit surface area, kg/m²·s
h_{fg} = latent heat of vaporization, J/kg
k = thermal conductivity of heater block, W/m·K
k_l = liquid thermal conductivity, W/m·K
l = distance between two thermocouples in the heater block, m
$\dot{m}_l$ = liquid mass flow rate, kg/s
N = rate of droplets impinging per unit area, $6V/(\pi d_{30}^3)$, /m²·s
N_t = total number of droplets in the spray in a sample time
q'' = heat flux, W/m²
q''_c = critical heat flux, W/m²
Re_D = Reynolds number, $\rho_l v D/\mu_l$
T_{sat} = saturation temperature, K
T_w = surface temperature, K
u_b = velocity of growing bubble surface, m/s
V = volume flow rate per unit area of heater, m³/m²·s
v = average spray droplet velocity, m/s
β = spreading ratio, d_d/d_{20}
ΔP_l = pressure drop across nozzle exit, Pa
ΔT = superheat, $T_w - T_{sat}$, K
δ = initial macrolayer thickness, m
μ_l = dynamic viscosity of liquid, N·s/m²
ρ_l = liquid density, kg/m³
ρ_v = vapor density, kg/m³
σ = surface tension, N/m

Presented as Paper 94-2010 at the AIAA/ASME 6th Joint Thermophysics and Heat Transfer Conference, Colorado Springs, CO, June 20–23, 1994; received June 24, 1994; revision received Feb. 14, 1995; accepted for publication Feb. 15, 1995.

*Engineer Associate, Department of Mechanical Engineering. Member AIAA.
†Professor, Department of Mechanical Engineering. Associate Fellow AIAA.
‡Professor, Department of Mechanical Engineering.
§Associate Research Professor, Department of Mechanical Engineering. Member AIAA.

Introduction

THE advantages of operating electronics at low temperatures have been enumerated in numerous studies.[1–4] However, even at low temperatures, high heat flux removal techniques will be needed for some superconducting circuits and high-voltage power conversion applications.

This has led to interest being focused on spray cooling as the high heat flux removal technique. Spray cooling with liquid nitrogen (LN2) has been used in the food storage industry to rapidly and efficiently freeze the perishable goods. Spray cooling with water has found use in cooling steel forgings and in continuous casting process. All of these uses, however, have involved surfaces with much higher temperature as compared to the fluid used for spray cooling (high superheats). At these temperatures the fluid does not wet the surface and the heat transfer is by the process of conduction through the thin film of vapor that exists between an impinging droplet and the hot surface. The phenomena involved in this form of spray cooling has been widely studied.[5,6] This form of spray cooling has a low heat transfer coefficient h, and thus, is not very useful for applications that involve high heat fluxes. However, the same spray is capable of providing extremely high heat transfer coefficients at low superheats.[7–9] If we compare spray cooling to the other cooling methods we find that the heat transfer coefficients are significantly higher. For instance, pool boiling with water has $h \sim 5 \times 10^4$ W/m²·K, while, for spray cooling using water, h over 5×10^5 W/m²·K has been observed.[8] Another major advantage of spray cooling is that much higher heat fluxes can be achieved at relatively low surface temperatures (i.e., high critical heat flux). Spray cooling with water has been shown to be capable of removing close to 10 MW/m² at temperatures lower than 140°C under normal surface conditions.[7–9] For very smooth surfaces heat fluxes higher than 10 MW/m² have been achieved at surface temperature lower than 105°C, using water as the coolant.[8]

Most of the earlier spray cooling research involved low heat fluxes and low fluid flow rates.[10,11] In the past few years a significant amount of work has been done in high heat flux spray cooling research.[7–9,12–14] The complexity of the phenomena involved have, however, frustrated attempts to successfully model the process. A comprehensive predictive correlation/model for spray cooling has not been available. A number of studies have attempted to correlate the spray cooling characteristics with the spray parameters.[15,16] However,

none of these correlations are very useful unless the same fluid and nozzle used in the study are being used. This is due to the fact that none of these studies compared different liquids and nozzles, and therefore, provided only simplistic correlations.

Hence, the main objective of this study is to obtain correlations for the heat transfer characteristics of spray cooling with liquid nitrogen. This is done by experimentally obtaining heat transfer data for LN2 spray cooling under different spray conditions. The results of these experiments have been reported in a previous study.[1] However, the spray parameters were unavailable at the time of that study. The spray parameters were measured as part of this study and are used in correlating the data reported earlier. The following sections describe the experimental setup and procedure, results, and correlations.

Experimental Setup and Procedure

The schematic diagram of the experimental setup is shown in Fig. 1. The experimental chamber contains the heater, nozzle, and view ports. The high-pressure LN2 dewar is used to supply liquid nitrogen to the nozzle. A heat exchanger between the dewar and the nozzle is used to subcool the high-pressure liquid down to about 78 K. Since the chamber is always maintained at atmospheric pressure, the liquid spraying out of the nozzle is always close to saturation if the upstream temperature is maintained at about 78 K (assuming isentropic expansion). All the lines were insulated with polyurethane foam to minimize heat gain. During preliminary experiments, it was found that, at low flow rates, it was very difficult to maintain a single phase fluid supply into the nozzle inlet, this resulted in violent pressure fluctuations and eventual disruption of flow. This happened because the heat gain into the line was sufficient to vaporize a part of the liquid flow at low flow rates. In order to overcome this problem, a bleed port was provided just prior to the nozzle. Thus, the total flow through the line could be maintained high enough to prevent vaporization. The bleed flow was vaporized by passing it through a long heat exchanger tube coil placed in a hot water bath. The bleed flow was continuously monitored by a mass flow meter measuring the flow rate of gaseous nitrogen exiting the heat exchanger.

The heater block is made out of oxygen-free copper. An electric cartridge heater inserted inside the copper block provides the heat. The heat transfer surface is a 1-cm^2 circle on the top of the block. The detailed design of the heater block is given in the previous study.[1] Two thermocouples in the copper block below the heat transfer surface measure the temperature gradient below the surface. The thermocouple distance was sufficient to enable extrapolation of average surface temperature even if a moderate lateral temperature gradient existed on the surface (a 5 K lateral gradient was used to obtain the design values). The heat flux and the average surface temperature is estimated from these thermocouple measurements. All surfaces of the heater block except the top are insulated using polyurethane foam (thermal conductivity: 0.035 W/m · K) to prevent heat loss. The heat loss from the block was estimated to be less than 2% with this insulation (based on calculations assuming that the outer surface of the insulation is at LN2 temperature). The heat input from the cartridge heater was determined by measuring the power input to the heater using a power transducer. This measurement was used to confirm the heat flux calculated from the temperature gradient and validate those calculations.

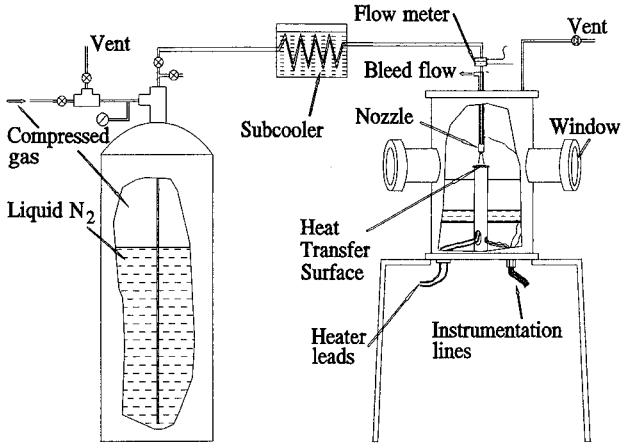

Fig. 1 Experimental setup.

In addition to those in the copper block, thermocouples were also placed on the insulation surface, inside the chamber, on the nozzle body, in-stream near nozzle inlet, in the subcooling heat exchanger, and on the chamber surface. The liquid flow rate to the nozzle is calculated by subtracting the bleed flow rate from the flow rate measured by an orifice-flow-meter. All of the thermocouples and the power transducer output were read by a Fluke Helios Plus data acquisition system connected to a personal computer.

An experimental run involved spraying the LN2 at a certain pressure and 78 K through the nozzle onto the heater surface. The roughness of the heater surface was measured before the heater was installed in the chamber, and also at the conclusion of the whole set of experiments. The average roughness R_a was measured by a surface profilometer (Surtronics 3P, Rank Taylor–Hobson, Ltd.), and was in the range of 0.05–0.15 μm, both before and after the experiments. The surface was cleaned with a very dilute solution of hydrochloric acid and then rinsed with deionized distilled water and propanol prior to each set of experiments. Before beginning the experiment, the chamber is flushed with nitrogen to expel any air or water vapor. The subcooling heat exchanger shell is filled with LN2 and the fluid is allowed to flow from the dewar to the nozzle. The bleed port is kept fully open until the line cools down to LN2 temperature. This is evidenced by the temperature of the nozzle reaching 78 K. The pressure of the dewar is then set at the desired value by venting the dewar or pressurizing it from a N2 gas cylinder. The bleed valve is adjusted until the bleed flow is as low as possible while still sufficient to maintain the nozzle temperature at 78 K. The nozzle height and alignment are adjusted to ensure that the spray covers the whole heat transfer surface and all the spray impinges the surface.

The power to the heater cartridge is then increased gradually until dryout of the surface occurs. After each step increase in power, sufficient time is allowed for all the temperatures to reach steady state. The power to the heater is cut off immediately following the dryout. Dryout is evidenced by the rapid increase in temperature readings of the two thermocouples inside the copper block. Upon dryout, the temperature of the surface usually reaches about 200 K because of the thermal inertia of the heater block. The data recording is continued until the surface temperature falls back to about 80 K under the same spray conditions. Although these cooldown readings are not at steady state, the correct heat flux and surface temperature can be estimated by correcting for the temperature transients. The cooldown readings provide the heat transfer characteristics for LN2 spray cooling in the Leidenfrost point region.

In general, a set of runs were taken consecutively until the LN2 in the dewar ran out, or, the nozzle had to be changed. The set of results presented here involved four nozzles: 1) TG0.3 (0.76 mm), 2) TG0.5 (0.61 mm), 3) TG0.7 (0.51 mm), and 4) FL#13 (0.38 mm) (the figures in parentheses indicate the nozzle orifice diameter for each nozzle). The TG series nozzles are full-cone pressure atomizing nozzles commercially available from Spraying Systems Co., Wheaton, IL. These nozzles have a flow swirler before the orifice that creates

turbulent flow for effective atomization. The FL#13 is a flat disc-shaped nozzle with radial grooves leading to the orifice (for creating turbulence).

The experiments were carried out for five to six different pressures for each nozzle (207, 276, 414, 552, 690, and 828 kPa). The nozzle inlet pressure was continuously monitored by a Bourdon gauge connected to the low-pressure side of the orifice-flow-meter. The spray cone for the FL#13 nozzle (about 40 deg) was much narrower than that for the TG series nozzles (about 60 deg). The nozzle height above the surface was varied to keep the surface covered with spray, all the experiments with TG series nozzles had approximately the same nozzle height: 1 cm; the height for the FL#13 nozzle was 1.6 cm. The nozzle height was adjusted such that the spray cone hit the whole surface and did not extend beyond it. All the nozzles used in this study had no nonuniformities in the angular direction (i.e., the spray cones always had a circular cross section). The spray parameters: droplet size distribution and velocity distribution were measured by a phase Doppler particle analyzer (PDPA). These parameters could be measured using the PDPA system through the windows provided on the experimental chamber.

The spray parameters of importance are the droplet size and velocity distribution at the heat transfer surface. These parameters were measured at appropriate distance from the nozzle exit (1 cm for TG nozzles and 1.6 cm for FL#13 nozzle). Thus, the droplet velocity and size distributions at various radial positions in the plane perpendicular to the nozzle axis were measured for each nozzle at the same flow conditions used in the heat transfer experiments.

Uncertainty Analysis

The heat flux is measured by using the temperature gradient readings provided by the two thermocouples in the copper block (using Fouriers's law: $q'' = k\Delta T/l$). Hence, the uncertainty in heat flux measurement is related to the uncertainty in the measurement of temperature difference between the two thermocouples in the copper block. The manufacturer specified uncertainty in the temperature measured by E-type thermocouples is 1.7 K. However, at a heat flux of 0 W/m^2 (at 78 K), the two thermocouples always read within ± 0.25 K. Thus, this is a better measure of the error in ΔT (note that this ΔT is not the superheat). The relative uncertainty in thermal conductivity of copper ($\Delta k/k$) is 0.02. The two thermocouples are located in holes that have a diameter of 0.5 mm each and are 16.5 mm apart (center-to-center distance). The relative uncertainty in distance between the thermocouples ($\Delta l/l$) is, therefore, 0.06. Hence, the maximum relative uncertainty in heat flux measurement comes to $0.08 + 0.25/\Delta T$. This uncertainty decreases with increase in ΔT. Near critical heat flux, the ΔT is usually on the order of 50 K. Thus, the uncertainty in CHF is close to $\pm 8\%$.

The surface temperature is calculated by extrapolation from the two thermocouple readings. The maximum uncertainty in surface temperature was found by calculations to be 3.0 K at a heat flux of 1500 kW/m^2. The nozzle pressure is measured by a gauge having a least count of 13.8 kPa (2 psig). Since the mass flow rate is estimated by using an orifice-meter, the uncertainty is composed of the error in pressure drop measurement and the error in discharge coefficient C_d. The differential pressure transducer has an uncertainty of 2%, and the uncertainty in C_d is about 3%. Thus, the uncertainty in mass flow rate is less than 5%.

Results and Discussion

Since most of the LN2 spray cooling heat transfer data used in this study was reported in a previous study,[1] the results of spray parameters measurements are presented first. The measurements were carried out by an Aerometrics PDPA system having the ability to measure the droplet size distribution and the velocity along a single flow direction. The velocity distribution data obtained during the experiments was very repeatable and easy to obtain. The same was not true for the droplet size distribution. Since the sprays produced during these experiments were very dense and consisted of very fine droplets, the PDPA system had a great difficulty in providing consistent data. Also, the very nature of optical measurements biases the instrument in favor of the larger droplets.

The dense nature of the spray prevented the droplet diameter data collection for high-pressure cases for all the nozzles. The reliability of the data is related to the validations/samples ratio. The PDPA system uses three in-line detectors to collect the phase shift data that is used to calculate the droplet size. Thus, it takes two readings of the phase shift of the Doppler signal, between the first and second, and, the second and third detector. If the readings do not match, more than one droplet was probably present in the probe volume and that sample is therefore rejected. Thus, the system provides a validations/samples ratio that is a measure of the reliability of the spray distribution characteristics measured. The validations/samples ratio for droplet diameter measurements was too low to be reliable in most cases. Even for the low-pressure sprays this ratio was as low as 0.6, i.e., almost half the data samples were rejected.

Since reliable data on the Sauter mean diameter d_{32} could not be obtained for the majority of cases, a correlation for d_{32} had to be used. Lefebvre[17] suggested a general correlation for d_{32} for pressure-atomizing-swirl nozzles based on extensive data and literature survey. This correlation, shown here as Eq. (1), underpredicts the d_{32} values measured experimentally in this study (but the trend of the data was correct). However, the reliability of those measurements was questionable, and therefore, the deviation showed by the correlation is not unreasonable. Table 1 shows the d_{32} values predicted by the correlation and the measured values (in parentheses) for some cases. The values of d_{32} calculated from the correlation were used for data reduction purposes:

$$d_{32} = 2.25\sigma^{0.25}\mu_l^{0.25}\dot{m}_l^{0.25}\Delta P_l^{-0.5}\rho_v^{-0.25} \quad (1)$$

The velocity distribution from the measurements was reasonably repeatable and could be considered reliable. The average velocities for the test cases, at the center of the spray, are shown in Table 1. The velocity distribution for any location was always Gaussian with a standard deviation of 2–4 m/s. The spray velocity as a function of the radial position in the spray was also obtained. In all cases, the velocity dis-

Table 1 LN2 spray parameters

Nozzle	Pressure, kPa	G, kg/m^{2}s	d_{32}, measured value, μm	Velocity, m/s
FL#13	276	16.9	21 (30–33)	16.0
	414	20.3	18 (23–27)	18.5
	552	23.3	16	20.3
	690	25.6	15	22.6
	828	27.8	14	24.2
TG0.3	276	20.6	22 (33–38)	14.0
	414	24.9	19	15.1
	552	28.4	17	18.3
	690	31.3	15	19.7
	828	34.1	14	21.0
TG0.5	207	37.3	29 (40–48)	15.4
	276	42.8	26	17.9
	414	51.4	22	21.8
	552	58.9	20	25.4
	690	65.0	18	28.5
	828	70.6	17	30.7
TG0.7	276	55.4	28	19.0
	414	66.7	24	21.6
	552	75.8	21	23.1
	690	82.8	19	24.8
	828	88.9	18	27.1

tribution was fairly constant for most of the spray, however, the velocity falls off very sharply close to the spray edge. This is probably due to the fact that the outermost droplets suffer significantly more drag compared to those inside the spray cone. The average velocity variation with the radial position was similar for all the nozzles used in this study. Hence, the mean velocity at the center can be considered as the representative velocity for a spray condition.

Before moving on to the heat transfer data, a brief discussion of spray cooling theory is presented to provide a better insight into the results. Figure 2 shows the probable mechanisms involved in spray cooling heat transfer. Convection heat transfer, evaporation from the film surface, nucleate boiling at the heater surface, and secondary nucleation are all thought to be involved in spray cooling. The intense convection caused by impinging droplets enhances the heat transfer between the heater surface and the free surface of liquid film and the heat transferred to the film surface goes towards evaporation of the fluid.

Nucleate boiling at the heater surface with premature bubble removal also helps in increasing the heat transfer coefficient. Since a spray with high-speed droplets is subjected on the liquid film surface, the bubbles growing in the liquid film cannot survive as long as those in a pool of liquid. Thus, the bubbles can break up at a very small size, even before the microlayer[18,19] is completely evaporated. This bypasses the much longer and less efficient growth period in pool boiling where the bubble has to grow slowly after microlayer evaporation in order to attain enough volume for the buoyancy forces to overcome the surface tension forces holding the bubble to the surface. The overall effect of this premature bubble break-up is to increase the total time the microlayer evaporation exists on a surface and thereby increase the heat transfer coefficient.

Finally, secondary nucleation,[20,21] which results from the entrapment of vapor bubbles by impinging liquid droplets, also plays an important role in spray cooling. The term secondary nucleation was coined to describe the nuclei from the vapor entrained by the re-entering droplets created by bubbles bursting out of the liquid film. Due to the lack of a better term and the fact that the phenomenon is similar whether the droplets originate from the liquid film, or from an external source (spray in this case), we refer to nucleation due to vapor entrained by the spray as secondary nucleation. Also, due to the very high number density of spray droplets impinging on the liquid film, the dominant source of this secondary nucleation is likely to be the spray itself. The heat transfer due to secondary nucleation would be less efficient as compared to microlayer evaporation since the thickness of liquid layer between a secondary nucleus and the heat transfer surface is larger than the microlayer thickness. Although it is conceivable that a bubble due to a secondary nucleus can get close enough to the heat transfer surface to permit microlayer evaporation, the time for this type of microlayer evaporation is unlikely to approach that experienced by a bubble originating from a surface cavity. Hence, it is safe to assume that bubbles originating from surface cavities remove heat more efficiently as compared to bubbles originating away from the surface.

The detailed results from the heat transfer experiments have been reported in a previous study.[1] For the purpose of discussion, a set of results from that study are provided here. Figure 3 shows the heat transfer characteristics of spray cooling with three different nozzles at the same inlet pressure (414 kPa) and similar surface roughnesses (R_a in the range: 0.05–0.15 μm).

As seen from Fig. 3, the heat transfer curves are made up of three distinct regions. The first is the low superheat region. Here, the heat transfer is probably dominated by forced convection with evaporation from the film surface and secondary nucleation. Nucleate boiling from the surface is relatively insignificant in the first region because surface nucleation requires a higher superheat under forced convection situations and would be noticeable by a distinct change in slope.[22] On the other hand, boiling due to secondary nucleation can exist from a very low superheat and would be undeterminable from the heat transfer curve in this case. As the superheat is increased, the slope of one of the curves shows a small jump at about 10 K superheat. This is probably due to a sudden increase in nucleate boiling from cavities on the heater surface (i.e., a substantial number of surface cavities are activated around this superheat). As mentioned earlier, nucleation from the surface cavities allows microlayer evaporation, and hence, higher heat transfer coefficient as compared to nuclei originating in the liquid film. Hence, this shift in slope could be attributed to the boiling from nucleation sites on the surface. Once the nucleate boiling from the heater surface increases, the same curve shows a definite shift upwards, this second region can be said to have a significant contribution by surface nucleation. However, since this did not occur for all the cases, it was felt that the change in slope for some of the cases could have been caused by undetectable changes in the heat transfer surface (presence of oxide layer). The final region is a flattening of the curve leading to the CHF, this is similar to the behavior seen in flow boiling situations. In order to investigate the effects of surface conditions, which seemed to play a role in the previous experiments, some experiments were conducted as part of the present study.

The roughness of the heat transfer surface was varied to investigate the effect of surface conditions. Three different surface roughnesses were tested. The average roughness R_a values of the test surfaces were: 0.05, 0.3, and 0.6 μm (measured with a Rank–Taylor 3P profilometer). Figure 4 shows the difference in heat transfer characteristics for the three surfaces. It is clear from the figure that the surface roughness

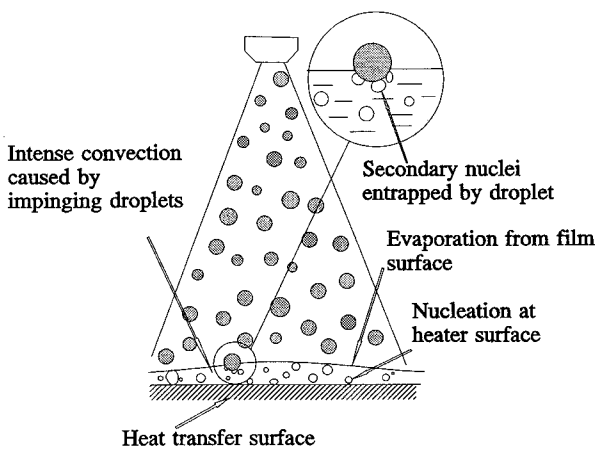

Fig. 2 Spray cooling.

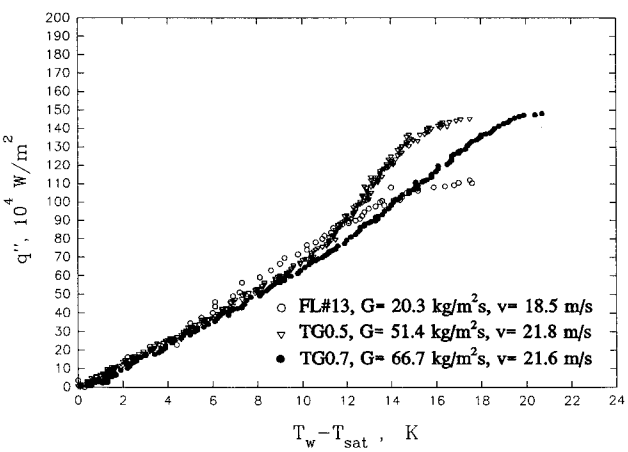

Fig. 3 Spray cooling heat transfer characteristics.

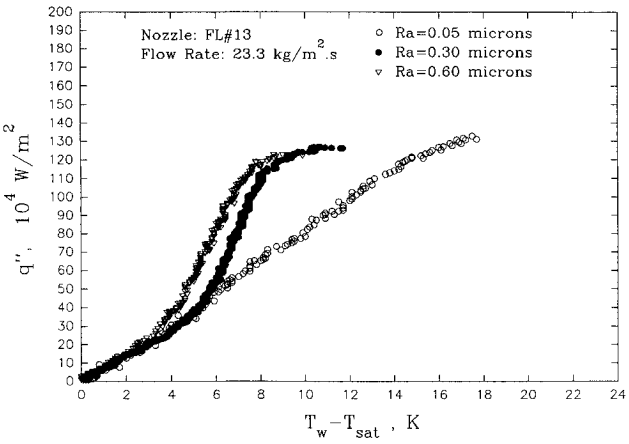

Fig. 4 Effect of surface roughness.

makes a significant difference in the heat transfer phenomena. Clearly, the smoothest surface shows no abrupt change in slope, whereas the two rougher surfaces show a significant shift in slope as superheat increases. The temperature at which this shift in slope occurs, decreases with increase in surface roughness. This is a clear indication of change in surface nucleation characteristics. As reported by numerous researchers, the temperature for onset of nucleate boiling decreases as the surface roughness increases. In the present case, this clearly points to the fact that the rougher surfaces show a significant contribution of surface nucleation while the smoothest surface does not. Since surface nucleation is much more efficient as compared to secondary nucleation and surface evaporation, the presence of surface nucleation causes a significant increase in the heat transfer rate for the rough surfaces. The smoothest surface continues to have the same heat transfer coefficient with increase in superheat. This indicates that the contribution of surface nucleation is small compared to that of secondary nucleation.

These results prove the speculation from the previous study that the shift in slope for some cases (as in Fig. 3) was due to small differences in surface conditions. This effect is especially significant for a highly wetting liquid like LN2. The surface nucleation cavities for the smooth surfaces are easily deactivated by flooding, and hence, the surface nucleation contribution is not significant for smooth surfaces.

As seen from Fig. 4, the critical heat flux (CHF) for the different surfaces is within a spread of 5%. Since the CHF is very sensitive to experimental conditions, this deviation is not so significant. Some other experiments conducted at other flow rates showed a slight increase in CHF for rougher surfaces. Hence, it was felt that the differences in CHF due to surface roughness did not show any significant trend. This leads us to the conclusion that the CHF is not significantly effected by the surface condition.

The trend for the effect of surface roughness is quite different from that reported by Pais et al.[8] for air-atomized water spray cooling. As reported in that study, the effect of roughness in spray cooling with air-atomized water is not significant until the surface is very smooth. For very smooth surfaces, the heat transfer coefficients and the CHFs were found to be much higher. The difference in trends is probably due to the method of spray application because Tilton[7] (pressure-atomized water spray) reported roughness effects similar to those in the present study. The difference for air-atomized spray probably arises due to the presence of the secondary gas (air) flow. The stagnation flowfield created by the airflow causes the thickness of the liquid film to decrease when the surface is very smooth; this reduces the thermal resistance from the heater surface to the film surface. This does not seem to happen in pressure atomized spray cooling due to the absence of the secondary gas flow. The secondary gas flow does two things. First, it thins and flattens the liquid film, and second, it reduces the partial vapor pressure on the film surface. These effects are absent in pressure-atomized spray cooling; hence, the liquid film is not expected to be very thin, and, therefore, the surface evaporation is less significant. This is probably the reason for the differences in the effect of surface roughness for these modes of spray application.

Since less than 30% of the liquid evaporates at the maximum heat flux for the case shown in Fig. 4, the CHF is not caused by a lack of liquid supply. There are two conditions under which the CHF mechanism can be similar regardless of surface condition. First, if the vapor generation at the surface is significant, the vapor flow can entrain the incoming droplets and prevent liquid replenishment on the surface. Second, if secondary nucleation is significant, the total bubble generation in the liquid film on the smoothest surface could approach the bubble generation due to surface nucleation on the rough surfaces. Thus, a vapor layer can form on the heater surface and the dryout may be controlled by the thin liquid layer (macrolayer) initially present below this vapor layer. This follows the macrolayer dryout model suggested by Haramura and Katto.[23]

The first condition is not very likely. If we assume that the vapor generated from the surface flows only upwards, the vapor velocity at CHF would be about 1.3 m/s. This is much lower than the average droplet velocities, hence, it is unlikely that the droplets can be entrained by the vapor flow. Thus, it is very likely that the bubble generation in the liquid film gives rise to CHF conditions. The exact CHF mechanism is not clear since the visualization in the liquid film formed by the spray is all but impossible. However, it is quite likely that the CHF occurs due to the dryout of the macrolayer. This hypothesis, the reasoning behind it, and the resulting CHF correlation, are explained in the following section.

Data Reduction and Correlation Development

One of the major difficulties in analyzing spray cooling lies in isolating the various spray parameters. The droplet velocity, diameter, and the volume flow rate are directly related to the nozzle pressure for a particular nozzle. This was the reason for selecting different nozzles for the study. The range of parameters for the LN2 study were, d_{32} = 14–29 μm, the velocity = 14–31 m/s, and the mass flow rate = 16.9–88.9 kg/m^{2}s.

Critical Heat Flux

The maximum effectiveness of the spray cooling (defined as $q''_c/h_{fg}G$) for the LN2 spray cooling study was never above 0.35, hence, the CHF was not caused by a lack of liquid (as is the case for low flow rate mist cooling situations). The CHF is caused by the inability of the liquid to reach the surface at a sufficient rate. The hypothesis for the dryout condition is presented in Fig. 5. As shown in the figure, the dryout condition occurs in the following sequence:

1) Increasing the rate of bubbles production in the liquid film gives rise to a larger vapor bubble (which may last for only a few microseconds due to the high rate of bombardment by spray droplets).

2) This vapor bubble is broken due to an impinging droplet (or due to the excessive internal pressure) and the liquid forming the upper layer of this bubble is blown away by the vapor flow.

3) The incoming droplets continue to wet the rapidly drying-out surface. The dryout will occur if the incoming droplets cannot wet the whole surface before the macrolayer dries.

The dryout condition can be written in mathematical form as Eq. (2). Here δ stands for the initial macrolayer thickness, d_d represents the average diameter of the disc formed by an impinging droplet ($d_d = \beta d_{20}$, where β is the spreading ratio), and N is the number of droplets hitting a unit area per unit time. Thus, Eq. (2) represents a balancing of the time required

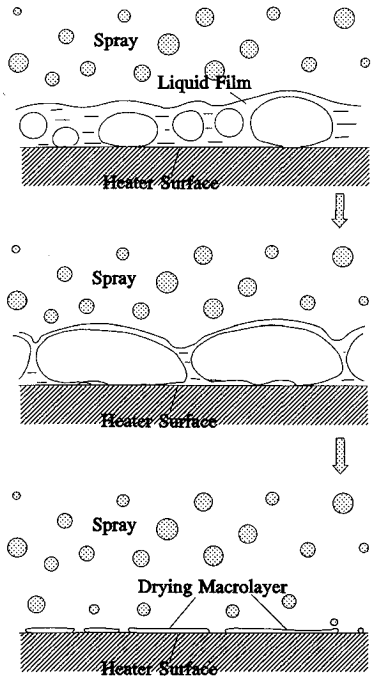

Fig. 5 Critical heat flux.

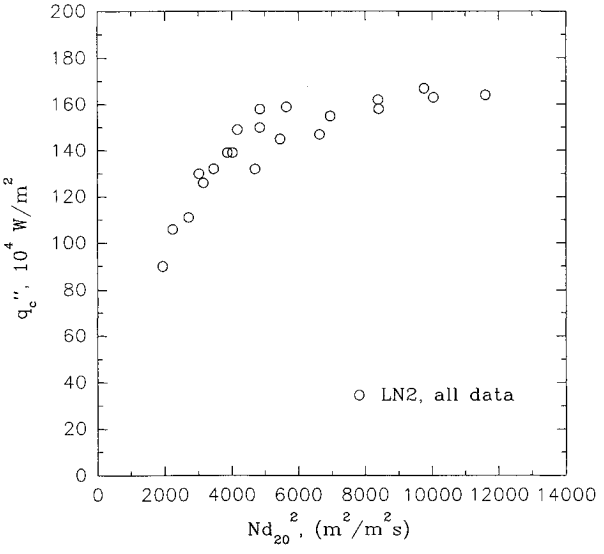

Fig. 6 Effect of Nd_{20}^2 on CHF.

to wet a unit area and the time required to evaporate the macrolayer of thickness δ initially present on that area:

$$1/N[(\pi/4)d_d^2] = \rho_l \delta h_{fg}/q_c'' \tag{2}$$

The experimental support for the previous hypothesis comes from two key observations. One, the second step in the model described is supported by an observation by Tilton,[7] where he reported that a large amount of droplets was expelled from the surface when the heat flux was close to the CHF. Second, the third statement is supported by experimental evidence shown in Fig. 6, which indicates the CHF dependence on the surface area impacted per second by the droplets. The data shown in the figure indicate that the CHF is a direct function of Nd_{20}^2 (proportional to the area wetted per second). Here, it should be noted that Nd_{20}^2 is equal to $6V/\pi d_{32}$. Hence, it is not necessary to determine d_{30} and d_{20} individually.

Based on Fig. 6 and the data reported by Tilton, there is sufficient evidence supporting the macrolayer dryout model. A correlation for CHF in liquid nitrogen spray cooling can be easily obtained from Fig. 6 alone. In order to obtain a general correlation, we considered data obtained by Tilton[7] (water spray on a horizontal surface), and Cho and Wu[16] (R-113 spray on a vertical surface). It should also be mentioned that for the purpose of this study, the d_{32} (and consequently Nd_{20}^2) values for both of these studies were calculated using Eq. (1).

The difficulty in the application of the macrolayer dryout model lies in the estimation of the initial thickness of the macrolayer. Haramura and Katto[23] obtained the macrolayer thickness based on the Helmholtz instability criterion for the vapor stems existing in the macrolayer. However, this situation does not seem very likely for very high heat flux cases. This is because the Helmholtz instability criterion indicates a very thin macrolayer (less than a micrometer thick if the Haramura and Katto model[23] is used) for the heat fluxes encountered in spray cooling. Vapor stems (and instability in those short stems, if they exist) in such a thin macrolayer seem unlikely. Another model for initial macrolayer thickness was proposed by Kumada and Sakashita.[24] Their model is based on the lateral coalescence of the vapor bubbles on a heated surface. They obtained the initial thickness of the macrolayer based on a number of dimensionless parameters. However, their model resulted in a very involved expression (containing a number of empirically determined indices) for macrolayer thickness. An attempt to use their model for obtaining a general correlation for spray cooling CHF was not successful. In this study we use dimensional analysis to obtain the initial macrolayer thickness.

The macrolayer is formed by the lateral coalescence of small bubbles that go on to form a bigger vapor layer that may exist for a very short time. Following the dimensional analysis of Kumada and Sakashita,[24] and considering only the significant dimensionless parameters, the initial macrolayer thickness can be written in nondimensional form as Eq. (3). The initial macrolayer thickness is related to the thickness of the liquid layer present below each individual bubble, which finally make up the vapor layer. The first term on the right-hand side (RHS) represents the ratio of the surface tension forces (which tend to keep the bubbles spherical), to the inertial forces (which act due to the rapid growth of the bubble and tend to keep the bubble in semispherical shape). The second term represents the density ratio, or the ratio of the mass of

$$\frac{\delta}{R_b} = C\left(\frac{\sigma R_b}{\rho_l R_b^2 u_b^2}\right)^i \left(\frac{\rho_l}{\rho_v}\right)^j \tag{3}$$

liquid displaced by an equal volume of vapor. The terms u_b (the velocity of the bubble surface), and R_b (average radius of the bubbles that coalesce to form the larger bubble below which the macrolayer exists) are unknown. Regarding R_b, it should be noted that δ should not be dependent on R_b. This is because the CHF for different surface conditions was found to be almost the same at very different superheats. This means that the macrolayer thickness was similar, although the nucleation conditions (and thereby, the number of bubbles) were quite different. Thus, δ should be independent of R_b. As most of the surface area is covered by bubbles prior to CHF, the velocity of bubble surface can be considered to be proportional to the rate of vapor production per unit area; i.e., we can write: $u_b = C_1 \cdot q_c''/\rho_v h_{fg}$. Substituting this value of u_b in Eq. (3) and recognizing that δ should be independent of R_b, we can obtain Eq. (4), which has only two unknown quantities, j and C_2.

$$\delta = C_2\left[\frac{\sigma}{\rho_l}\left(\frac{\rho_v h_{fg}}{q_c''}\right)^2\right]\left(\frac{\rho_l}{\rho_v}\right)^j \tag{4}$$

Substituting δ from Eq. (4) into Eq. (2), we obtain the

general form of the CHF correlation, Eq. (5). The unknowns β and C_2 are absorbed in C_3. This equation requires data

$$\frac{q''_c}{\rho_v h_{fg}} = C_3 \left(\frac{\sigma}{\rho_l} Nd_{20}^2\right)^{1/3} \left(\frac{\rho_l}{\rho_v}\right)^k \tag{5}$$

for only two different liquids (i.e., two values of the density ratio) for obtaining k and C_3. Here, the data for LN2 and water were used. Both of these data sets involved horizontal heaters of 1 cm^2, the heater surface for the water study was square in shape, while that for the LN2 study was circular. The data from the R113 study was not used in developing the correlation since that study was performed on a vertically oriented surface.[16] It has been reported by Choi and Yao[25] that the CHF in spray cooling is dependent on the surface orientation. They found that the vertically oriented surface exhibited higher CHFs. There is very little data available for vertical surfaces, therefore, we limit this correlation to horizontal surfaces only. The probable reasons for higher CHFs from vertical surfaces are discussed later. The final correlation for CHF, obtained using LN2 and water data, is shown in Eq. (6). The comparison of the correlation to various data is shown in Fig. 7:

$$\frac{q''_c}{\rho_v h_{fg}} = 0.31 \left(\frac{\sigma}{\rho_l} Nd_{20}^2\right)^{1/3} \left(\frac{\rho_l}{\rho_v}\right)^{0.5} \tag{6}$$

where

$$Nd_{20}^2 \equiv 6V/(\pi d_{32})$$

It should be noted that the spreading ratio β was assumed to be constant. This proved to be suitable for the range of data considered here, but, it may not hold for very low droplet Weber numbers (all cases considered in this study had droplet Weber numbers exceeding 100). In the range of data considered in this study, no correlation between β and the droplet Weber number could be found. Another point that can be noted is that the form of this correlation corresponds almost exactly to that obtained if Haramura and Katto's model for initial macrolayer thickness is used.

Although the R113 data was not used in obtaining the correlation, the data is only higher than the correlation by about 30%. This agrees with the fact that for a vertically oriented surface, the CHF is higher.[25] The other data points are quite well-compressed within a ±20% band. The reason for a vertical surface having higher CHFs is difficult to determine. It could be due to a number of reasons, among them: a vertical surface may have a thicker macrolayer; or, the liquid feed due to gravity may influence the CHF; or, some of the liquid blown away by exploding vapor bubbles may be re-entrained in the spray due to the horizontal orientation of the spray.

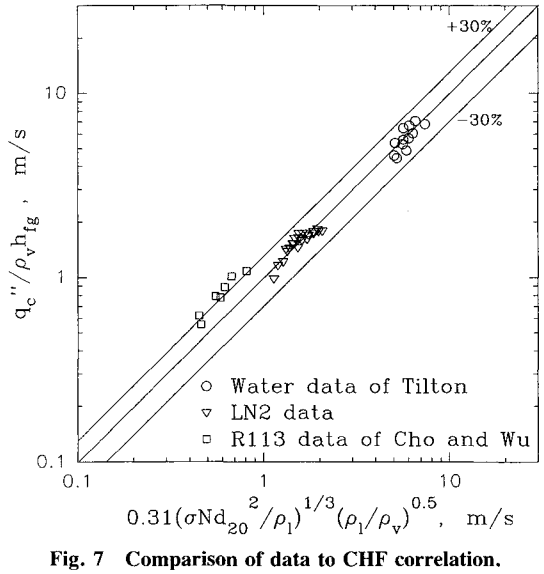

Fig. 7 Comparison of data to CHF correlation.

Cho and Wu[16] had successfully correlated their CHF data to the spray velocity. In fact, regarding all the data considered here, it is worth noting that the spray velocity v correlates the individual liquid data for LN2 and R113 reasonably well (water data shows only a weak dependence on v). However, the degree of dependence on velocity is different for each liquid, and thus, no general correlation involving the spray velocity was as successful as Eq. (6). Furthermore, no theoretical basis for correlating spray cooling CHF with the spray velocity could be found; whereas, the CHF model presented before is quite reasonable.

Heat Flux

Due to the lack of understanding of the fundamental processes involved in spray cooling, it is difficult to carry out the data reduction for heat flux. The difficulty lies in selecting the proper nondimensional variables to describe the spray process. Previous researchers have mostly used the droplet Weber number to correlate the heat transfer characteristics. The heat transfer rate due to the impact of single droplets has been shown to be a strong function of the droplet Weber number. However, the droplet Weber number alone cannot describe the spray cooling phenomena due to the presence of multiple droplets.

To begin, the nondimensional heat flux parameter is defined as $q''C_l D/h_{fg}k_l$. This is essentially the Nusselt number multiplied by nondimensional temperature difference represented by $C_l\Delta T/h_{fg}$. As explained earlier, the heat transfer rate dependence on the temperature difference is a very strong function of the surface roughness. The correlation of heat transfer rate with surface roughness is beyond the scope of this study. Hence, the heat transfer correlation for the smoothest surface only is attempted here. This is adequate because most electronic surfaces can be classified as smooth ($R_a < 0.1$ μm). Since a departure from the heat transfer curve for the smooth case was observed for some cases of the data set, the whole data set cannot be used in the correlation. Thus, only the surface roughness independent section of the curves were used in the correlation for heat transfer rate, this involved superheats lower than 8 K for all cases.

The first step was to correlate the temperature dependence of the heat transfer rate. The nondimensional parameter $C_l\Delta T/h_{fg}$ was used to correlate the temperature dependence of the heat flux, the best-fit exponent was 1.12. The other parameter that is important in heat transfer is the Reynolds number. The velocity in the liquid film is unknown, hence, the Reynolds number is not obvious. However, the velocity in the liquid film has to be closely related to the velocity of the spray droplets. Thus, we write the Reynolds number as $\rho_l v D/\mu_l$.

Another parameter that should have an effect on spray cooling heat transfer is the liquid film thickness. A thinner liquid film allows higher evaporation from the liquid surface and also permits the secondary nuclei to get closer to the heater surface. However, the liquid film thickness cannot be easily estimated. Hence, we define nondimensional velocity ratio V/v and droplet diameter ratio d_{32}/D. The velocity ratio is one of the factors that controls the liquid film thickness. As the spray droplet velocity v increases for the same overall flow rate per unit area V, the liquid film should be thinner due to the higher momentum of the incoming liquid. On the other hand, if the amount of incoming liquid V is increased keeping the droplet velocity the same, we should expect a thicker liquid film. The droplet diameter to surface diameter ratio d_{32}/D also influences film thickness. As the spray droplet size decreases, one would expect a thinner liquid film.

Using the nondimensional parameters defined above, the correlation for the spray cooling heat flux can thus be written

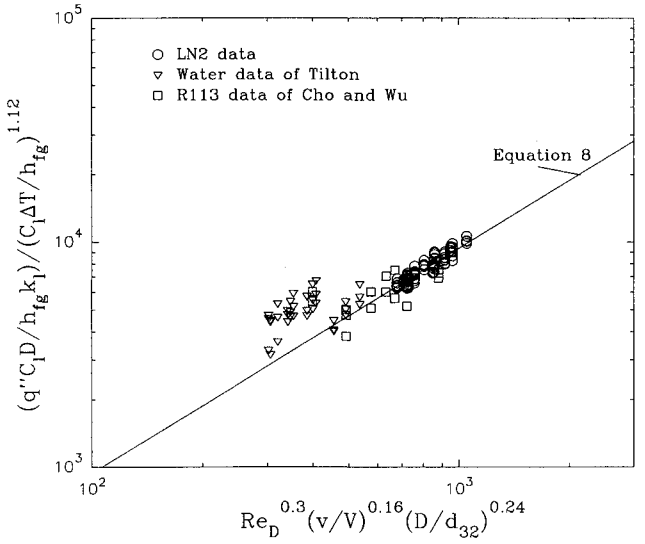

Fig. 8 Heat flux correlation.

as Eq. (7). The exponents m, n, and p along with the coefficient C_4 were determined from a best fit of the data. Hence, we finally get the correlation for heat flux as Eq. (8).

The comparison of the correlation to the experimental data is shown on Fig. 8. As seen from the figure, the agreement with the LN2 data is quite good. This suggests that the

$$\frac{q''C_lD}{h_{fg}k_l} = C_4 Re_D^m \left(\frac{V}{v}\right)^n \left(\frac{d_{32}}{D}\right)^p \left(\frac{C_l\Delta T}{h_{fg}}\right)^{1.12} \quad (7)$$

$$\frac{q''C_lD}{h_{fg}k_l} = 9.4 Re_D^{0.3} \left(\frac{v}{V}\right)^{0.16} \left(\frac{D}{d_{32}}\right)^{0.24} \left(\frac{C_l\Delta T}{h_{fg}}\right)^{1.12} \quad (8)$$

nondimensional numbers selected for the correlation are sufficient for the range of spray conditions in the LN2 study. The Reynolds number has the maximum influence on the heat flux. The D/d_{32} ratio and v/V ratio also have significant influence, thus, showing the importance of the liquid film thickness in spray cooling.

Again, it should be noted that this correlation applies only to liquid nitrogen spray cooling on smooth surfaces ($R_a < 0.1$ μm). A general correlation for heat flux was not attempted due to the lack of available data for liquids other than water in similar geometric configuration. Water is not a very good wetting liquid, hence, surface nucleation could exist from low superheats. Also, the water data was obtained at varying subcooling that was not reported. The data for other liquids were obtained for different geometries (R113 study[16]) or the spray parameters were not available.[15] Also, a better grasp of the factors influencing the liquid film thickness is needed. Hence, a general correlation for heat flux was not attempted. However, for the purpose of comparison, the heat flux data for water and R113 are also included in Fig. 8. As seen from the figure, these data are also quite well-compressed by the correlation. However, the Y value levels off with a decrease in X value. This may suggest that the heat transfer coefficient is more or less a property of the liquid at low X values. However, the data are not sufficient to make any conclusions. More data is required before a general correlation can be attempted.

Conclusions

Spray cooling is not a well-understood process. The purpose of this study was to obtain design correlations for the heat flux and the CHF for LN2 spray cooling. This study used the experimental heat transfer data from a recent study by the same authors and spray parameter data obtained during this study to obtain correlations for LN2 spray cooling process.

As part of this study, experiments were conducted to observe the effect of surface roughness. The rougher surfaces provided significantly higher heat transfer rates. This was attributed to the significant contribution of surface nucleate boiling for rougher surfaces. The smoothest surface had negligible surface nucleation and the main contribution to heat transfer was probably from secondary nucleation.

The CHF was deemed to be caused by the dryout of the macrolayer that is formed below the coalesced vapor bubbles in the liquid film. A general empirical correlation was obtained for CHF. This correlation showed very good agreement to previous data for water and R113 (although the data for R113 was not used in obtaining the correlation). The rate of surface wetted by the spray (i.e., the product of the rate of droplets impinging the surface and the area of the droplets) was found to be the main parameter influencing the CHF. A correlation was also developed for the heat flux in LN2 spray cooling. This correlation showed a dependence of the heat flux on the spray velocity and the droplet diameter.

Acknowledgments

This work was supported by Wright–Patterson Air Force Base, Ohio, Contract F33615-91-C-2152. Jeff Brown was the Technical Monitor. The assistance of Austin Pyle and Sylvan Ferrell from the workshop is also appreciated.

References

[1]Sehmbey, M. S., Chow, L. C., Hahn, O. J., and Pais, M. R., "Spray Cooling of Power Electronics at Cryogenic Temperatures," *Journal of Thermophysics and Heat Transfer*, Vol. 9, No. 1, 1995, pp. 123–128.

[2]Nisenhoff, M., "Superconducting Electronics: Current Status and Future Prospects," *Cryogenics*, Vol. 28, No. 1, 1988, pp. 47–56.

[3]Van Duzer, T., "Superconductor-Semiconductor Hybrid Devices, Circuits and Systems," *Cryogenics*, Vol. 28, No. 8, 1988, pp. 527–531.

[4]Mueller, O., "Cryogenic Power Conversion: Combining HT Superconductors and Semiconductors," *Superconductivity and Its Applications*, edited by Y. H. Kao, A. E. Kaloyeros, and H. S. Kwok, American Inst. of Physics, New York, 1991, pp. 746–759 (AIP 251).

[5]Deb, S., and Yao, S. C., "Heat Transfer Analysis of Impacting Dilute Spray on Surfaces Beyond the Leidenfrost Temperature," American Society of Mechanical Engineers National Heat Transfer Conf., Paper 87-HT-1, Pittsburgh, PA, 1987.

[6]Awonorin, S. O., "Film Boiling Characteristics of Liquid Nitrogen Sprays on a Heated Plate," *International Journal of Heat and Mass Transfer*, Vol. 32, No. 10, 1989, pp. 1853–1864.

[7]Tilton, D. E., "Spray Cooling," Ph.D. Dissertation, Univ. of Kentucky, Lexington, KY, 1989.

[8]Pais, M. R., Chow, L. C., and Mahefkey, E. T., "Surface Roughness and Its Effects on the Heat Transfer Mechanism in Spray Cooling," *Journal of Heat Transfer*, Vol. 114, No. 1, 1992, pp. 211–219.

[9]Sehmbey, M. S., Pais, M. R., and Chow, L. C., "A Study of Diamond Laminated Surfaces in Evaporative Spray Cooling," *Thin Solid Films*, Vol. 212, Nos. 1–2, 1992, pp. 25–29.

[10]Toda, S., "A Study of Mist Cooling. 2nd. Report: Theory of Mist Cooling and Its Fundamental Experiments," *Heat Transfer Japanese Research*, Vol. 3, No. 1, 1974, pp. 1–44.

[11]Bonacina, C., Comini, G., and Del Giudice, D., "Evaporation of Atomized Liquids on Hot Surfaces," *Letters in Heat and Mass Transfer*, Vol. 2, No. 5, 1975, pp. 401–406.

[12]Yang, J., Chow, L. C., Pais, M. R., and Ito, A., "Liquid Film Thickness and Topography Determination Using Fresnel Diffraction and Holography," *Journal of Experimental Heat Transfer*, Vol. 5, No. 3, 1992, pp. 239–252.

[13]Sehmbey, M. S., Pais, M. R., and Chow, L. C., "Effect of Surface Material Properties and Surface Characteristics in Evaporative Spray Cooling," *Journal of Thermophysics and Heat Transfer*, Vol. 6, No. 3, 1992, pp. 505–512.

[14]Yang, J., Pais, M. R., and Chow, L. C., "Critical Heat-Flux Limits in Secondary Gas Atomized Liquid Spray Cooling," *Journal of Experimental Heat Transfer*, Vol. 6, No. 1, 1993, pp. 55–67.

[15]Ghodbane, M., and Holman, J. P., "Experimental Study of Spray

Cooling with Freon-113," *International Journal of Heat and Mass Transfer*, Vol. 34, Nos. 4/5, 1991, pp. 1163–1174.

[16]Cho, C. S. K., and Wu, K., "Comparison of Burnout Characteristics in Jet Impingement Cooling and Spray Cooling," *National Heat Transfer Conference* (Houston, TX), HTD-Vol. 96, 1988, pp. 561–567.

[17]Lefebvre, A. H., *Atomization and Sprays*, Hemisphere, New York, 1989, Chap. 6.

[18]Cooper, M. G., and Lloyd, J. P., "Transient Local Heat Flux in Nucleate Boiling," *Proceedings of the 3rd International Heat Transfer Conference* (Chicago, IL), Vol. 3, Science Press, Ephrato, PA, 1966, pp. 193–203.

[19]Mesler, R., "A Mechanism Supported by Extensive Experimental Evidence to Explain High Heat Fluxes Observed During Nucleate Boiling," *AIChE Journal*, Vol. 22, No. 2, 1976, pp. 246–252.

[20]Mesler, R., and Bellows, W. S., "Explosive Boiling: A Chain Reaction Involving Secondary Nucleation," *ASME Proceedings of the 1988 National Heat Transfer Conference*, HTD-96, Vol. 2, 1988, pp. 487–491.

[21]Mesler, R. B., "Improving Nucleate Boiling Using Secondary Nucleation," *Pool and External Flow Boiling*, edited by V. K. Dhir and A. E. Bergles, American Society of Mechanical Engineers, New York, 1992, pp. 43–47.

[22]Rohsenow, W. M., "Boiling," *Handbook of Heat Transfer Fundamentals*, edited by W. M Rohsenow, J. P. Hartnett and E. N. Ganić, 2nd ed., McGraw–Hill, New York, 1985, Chap. 12.

[23]Haramura, Y., and Katto, Y., "A New Hydrodynamic Model of Critical Heat Flux Applicable Widely to Both Pool and Forced Convection Boiling on Submerged Bodies in Saturated Liquids," *International Journal of Heat and Mass Transfer*, Vol. 26, No. 2, 1983, pp. 389–399.

[24]Kumada, T., and Sakashita, H., "Proposed Model for Kutateladze Correlation and New Correlation of CHF," *Pool and External Flow Boiling*, edited by V. K. Dhir and A. E. Bergles, American Society of Mechanical Engineers, New York, 1992, pp. 177–183.

[25]Choi, K. J., and Yao, S. C., "Mechanism of Film Boiling Heat Transfer of Normally Impacting Spray," *International Journal of Heat and Mass Transfer*, Vol. 30, No. 2, 1987, pp. 311–318.